analytical chemistry

Article

pubs.acs.org/ac

"Wave" Signal-Smoothing and Mercury-Removing Device for Laser Ablation Quadrupole and Multiple Collector ICPMS Analysis: Application to Lead Isotope Analysis

Zhaochu Hu,*[,†,‡] Wen Zhang,[†] Yongsheng Liu,[†] Shan Gao,[†] Ming Li,[†] Keqing Zong,[†] Haihong Chen,[†] and Shenghong Hu[†]

[†]State Key Laboratory of Geological Processes and Mineral Resources, China University of Geosciences, Wuhan 430074, People's Republic of China

[‡]The Beijing SHRIMP Center, Institute of Geology, Chinese Academy of Geological Sciences, Beijing 102206, People's Republic of China

ABSTRACT: A novel "wave" signal-smoothing and mercury-removing device has been developed for laser ablation quadrupole and multiple collector ICPMS analysis. With the wave stabilizer that has been developed, the signal stability was improved by a factor of 6.6−10 and no oscillation of the signal intensity was observed at a repetition rate of 1 Hz. Another advantage of the wave stabilizer is that the signal decay time is similar to that without the signal-smoothing device (increased by only 1−2 s for a signal decay of approximately 4 orders of magnitude). Most of the normalized elemental signals (relative to those without the stabilizer) lie within the range of 0.95−1.0 with the wave stabilizer. Thus, the wave stabilizer device does not significantly affect the aerosol transport efficiency. These findings indicate that this device is well-suited for routine optimization of ICPMS, as well as low repetition rate laser ablation analysis, which provides smaller elemental fractionation and better spatial resolution. With the wave signal-smoothing and mercury-removing device, the mercury gas background is reduced by 1 order of magnitude. More importantly, the ^{202}Hg signal intensity produced in the sulfide standard MASS-1 by laser ablation is reduced from 256 to 0.7 mV by the use of the wave signal-smoothing and mercury-removing device. This result suggests that the mercury is almost completely removed from the sample aerosol particles produced by laser ablation with the operation of the wave mercury-removing device. The wave mercury-removing device that we have designed is very important for Pb isotope ratio and accessory mineral U−Pb dating analysis, where removal of the mercury from the background gas and sample aerosol particles is highly desired. The wave signal-smoothing and mercury-removing device was applied successfully to the determination of the ^{206}Pb/^{204}Pb isotope ratio in samples with low Pb content and/or high Hg content.

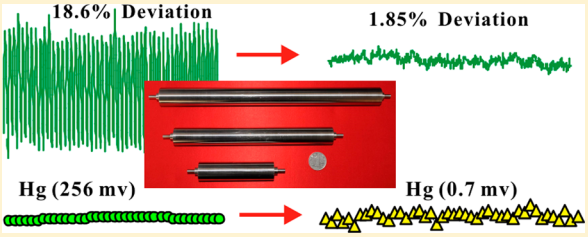

Laser ablation (LA) is becoming one of the most important technologies for direct solid sampling in analytical chemistry.[1−4] In LA-ICPMS analysis, it is well know that the sample position in the ablation cell influences the signal stability significantly in one volume cell.[5] In addition, laser ablation produced signals change quickly with time during single-hole ablation at a high repetition rate, which makes it difficult to optimize the instrumental parameters for ICPMS or multiple-collector ICPMS (MC-ICPMS) analysis.[6] For dating 5 μm zircon metamorphic rims, a lower laser ablation repetition rate such as 1 Hz is required.[6,7] Elemental fractionation is also significantly reduced at a lower laser ablation repetition rate, because it is strongly related to the depth-to-diameter ratio of the ablation crater.[8] However, a lower repetition rate results in an unstable signal that deteriorates the analytical precision. Due to the sequential nature of some ICPMS analysis (only one m/z value is detected at any one time), this may also lead to undesired spectral skew when certain dwell times are chosen during data acquisition.[9] Spectral skew is an error in relative signal levels for several m/z values across a transient signal that arises from the need to scan a spectrum while the input sample concentration is changing.[9] This is especially true for the recently designed volume-optional and low-memory (VOLM) chamber,[10] Laurin two-volume ablation cell,[11] low dispersion high capacity sample cell,[12] and laminar flow ablation cell,[13] whose cell-related memory effects are significantly reduced. To overcome these problems, Tunheng and Hirata[14] developed novel baffled-type and cyclone-type signal-smoothing devices. These stabilizers can provide a smoother signal at a repetition rate of 2 Hz, but the washout time can become significantly longer (approximately 20−40 s), and the resulting signal intensity is 15−20% lower. A "squid" signal smoothing device (Laurin Technic, Australia) has been designed to produce smooth signals even at very low laser repetition rates down to 1 Hz.[11] This squid signal-smoothing device splits the carrier gas (He + Ar) and sample aerosol line into 10 tubes with optimally differing lengths. After recombination into one gas line, a

Received: October 7, 2014
Accepted: December 16, 2014
Published: December 16, 2014

DOI: 10.1021/ac503749k
Anal. Chem. 2015, 87, 1152−1157

smoothed signal is produced. However, the washout time is improved by a factor of 2.2 (from 4 to 9 s for a signal decay of 5 orders of magnitude). Hu et al.[6] have developed a simple "wire" signal-smoothing device for LA-ICPMS analysis. With this wire signal-smoothing device, no oscillation of the signal intensity was observed, even at a repetition rate of 1 Hz. This wire signal-smoothing device has been used successfully for high spatial resolution U−Pb dating in zircon at low repetition rates of 1−2 Hz. Compared to other signal-smoothing devices, the significant advantage of the wire smoothing device is that the signal washout time is similar to that without the signal-smoothing device. However, the wire stabilizer device acts as a "particle filter" to a certain extent because the resulting signal intensity achieved with the stabilizer is lower than that without the stabilizer (10−30%). From the above observation, the trade-off between signal intensity and washout time is clearly a matter of compromise, which should be carefully considered during the design of the signal-smoothing device.

Lead isotope analysis in glass, sulfide minerals, and feldspar and U−Pb dating of accessory minerals (e.g., zircon) are very popular applications of LA-MC-ICPMS/LA-ICPMS in the earth sciences.[15−20] For correction of common Pb using the ^{204}Pb intensity in accessory minerals U−Pb dating, a small variation in the ^{204}Pb intensity can produce a large uncertainty in signal intensities for radiogenic ^{207}Pb and ^{206}Pb components.[21] Precise determination of the signal intensity of ^{204}Pb is thus highly important. However, ^{204}Pb has the lowest isotopic abundance and shares an isobaric interference with ^{204}Hg. Reduction of the mercury background in the ICPMS instrument is thus highly desirable. Mercury may be present in the Ar and He gases. Reduction of the Hg signal can be achieved by filtering the Ar and He gas using activated charcoal,[19] gold-coated sand,[20] or gold-coated glass wool.[22] A reduction of approximately 50% in Hg signal is achieved by using these devices. Hirata et al.[21] have developed a novel Hg-trapping device using an activated charcoal. Higher reduction efficiency of Hg signals was obtained with a larger volume of activated charcoal. For example, the Hg signals were reduced by a factor of 3 with a volume of charcoal filter of 200 mL. However, too high a volume of charcoal filter (e.g., 400 mL) resulted in lowering the signal intensity of Pb and U (approximately 40%). Aside from Ar and He gases, Hg also may be present in many mineral samples such as sulfides. Thus, removing Hg from laser ablation produced sample aerosol particles during lead isotope and U−Pb dating analysis is also highly desirable.

In this study, we have designed a novel "wave" signal-smoothing and mercury-removing device for laser ablation ICPMS analysis. The performance of the "wave" signal-smoothing and mercury-removing device was evaluated on the basis of the signal stabilities, signal intensities, washout time, and reduction efficiency of Hg. In the end, we applied this device to lead isotope analysis in sulfides and glasses by using laser ablation MC-ICPMS.

EXPERIMENTS

Instrumentation. Experiments were conducted using an Agilent 7500a ICPMS instrument (Agilent Technology, Tokyo, Japan) and a NEPTUNE Plus MC-ICPMS instrument (Thermo Fisher Scientific, Germany), which are connected to a GeoLas 2005 excimer ArF laser ablation system (Lambda Physik, Göttingen, Germany) at the State Key Laboratory of Geological Processes and Mineral Resources, China University of Geosciences in Wuhan. The standard ablation cell in the GeoLas 2005 system is a closed design cell and consists basically of a cylinder with a volume of approximately 51 cm^3 with an inlet nozzle (i.d. < 0.5 mm) and a gas outlet (i.d. = 1.8 mm). The energy density of the laser ablation that was used in this study was 5.0 J cm^{-2}. Helium was used as the carrier gas within the ablation cell and was merged with argon (makeup gas) after the ablation cell. Details of the instrumental operating conditions and measurement parameters are summarized in Table 1.

Table 1. Summary of the Operating Conditions Used for LA-ICPMS Measurements

GeoLas Laser Ablation System	
wavelength	193 nm, excimer laser
repetition rate	1, 6, and 8 Hz
pulse length	15 ns
energy density	5 J cm^{-2}
spot size	44, 60, and 90 μm
ablation cell gas	helium
makeup gas	argon
Agilent 7500a ICPMS	
rf power	1350 W
plasma gas flow rate	14.0 l min^{-1}
auxiliary gas flow rate	1.0 l min^{-1}
sampling depth	5.0 mm
ion optic settings	typical
dwell time per isotope	10 ms
detector mode	dual
NEPTUNE Plus	
rf power	1250 W
plasma gas flow rate	16.0 l min^{-1}
auxiliary gas flow rate	0.9 l min^{-1}
instrument resolution	400 (low)
block number	1
no. of cycles of each block	200
integration time	0.524 s

Wave Signal-Smoothing and Mercury-Removing Device. Figure 1 illustrates the schematic diagram of the wave signal-smoothing and mercury-removing device (a) and the connection position of the smoother in the LA-ICPMS system (b). The wave device essentially consists of a stainless steel cylinder filled with nine smoothing elements, with a volume of approximately 94 cm^3. Each smoothing element consists of seven intersecting corrugated plates (thickness 0.15 mm, corrugation angle 45°, wave height 4 mm, pitch of waves 7 mm) (Figure 1a). The length of seven corrugated plates is fixed at 30 mm. The widths of the seven corrugated plates are 9, 14, 18, 20, 18, 14, and 9 mm. In position A, only the He carrier gas flows through the stabilizer, whereas, in position B, both the He carrier gas and the Ar makeup gas flow through the stabilizer.

The surface of all the corrugated plates and the inner surface of the stainless steel cylinder were coated with ultrapure gold. The thickness of the gold coating is approximately 10 μm. The mercury in the carrier gas is expected to be trapped by the gold during transport through the wave stabilizer, in which the mercury frequently collides with the gold surface of the corrugated plates and the stainless steel cylinder.

DOI: 10.1021/ac503749k
Anal. Chem. 2015, 87, 1152−1157

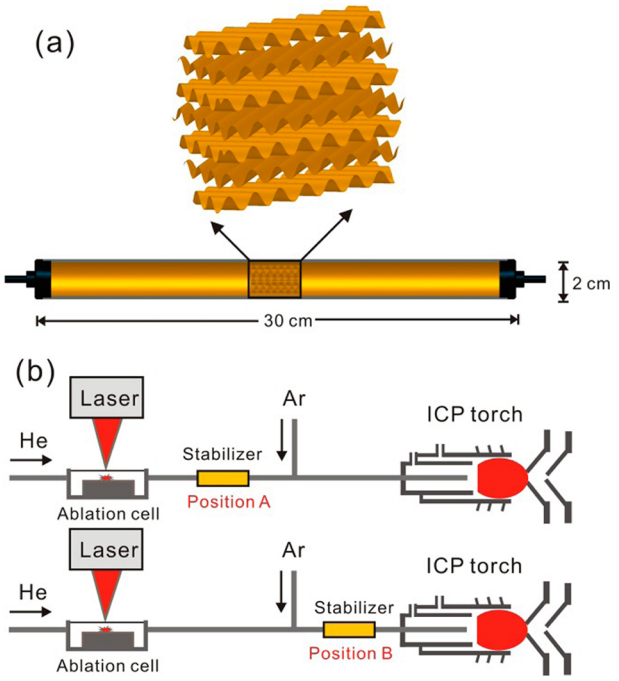

Figure 1. Schematic diagram of (a) the wave signal-smoothing and mercury-removing device and (b) the connection position of the smoother (position A or B) in the LA-ICPMS system. In position A, only the helium carrier gas flows through the stabilizer. In position B, both the helium carrier gas and the argon makeup gas flow through the stabilizer.

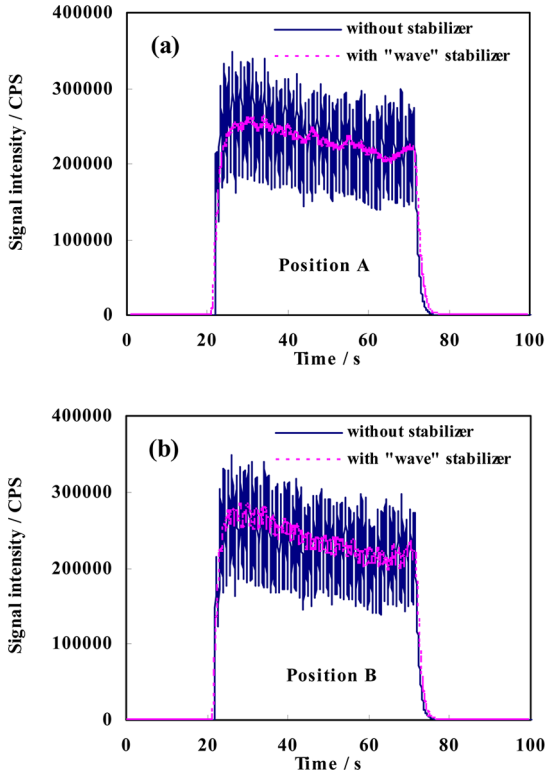

Figure 2. Uranium signal profile produced by continuous laser ablation without and with the wave device in position A (a) and position B (b). Signals were acquired using a repetition rate of 1 Hz and a spot size of 60 μm in NIST 610.

RESULTS AND DISCUSSION

Effect on the Signal Stability. Figure 2 shows the U signal profile produced by continuous ablation of the NIST SRM 610 glass at a repetition rate of 1 Hz and a spot size of 60 μm with and without the wave device at positions A and B. It can be seen that a smooth signal is obtained even at a repetition rate of 1 Hz by using the wave device. The stability of the U signal is improved from 18.6% to 2.81% and 1.85% for the wave device at positions A and B, respectively. The magnitude of the variability was calculated by subtracting the mean intensity estimated by the exponential decay pattern.[14] When the laser ablation produced aerosol particles are transported into the wave device, the aerosol stream is divided into many parts and deflected in different directions by the first smoothing elements, and these different aerosol parts continue to recombine and reseparate while passing through another eight smoothing elements. The different traveling pathways of the laser ablation produced sample aerosol particles in the wave device which lead to different exit times, defined as the time needed for the aerosol particles to travel through the stabilizer, that ultimately contribute to the stabilization. As shown in Figure 2, the stability of the U signal intensity in position A (1.85%) is better than that in position B (2.81%). This should be attributed to the reduced residence time of the sample aerosol particles in wave stabilizer in position B than that in position A due to the increased carrier gas flow rate in position B (He + Ar), which subsequently reduces the difference in exit time for the different parts of the sample aerosol in the stabilizer. This result also suggests that the expected improvement of signal smoothing by the mixing of He and Ar in the wave stabilizer is limited, which cannot compensate for the reduced smoothing effect due to the reduced exit time difference among the different aerosol particles in position B (He + Ar).

Effect on the Washout Time. The washout time refers to the time required for the signal to drop back to background levels after cessation of ablation. For high spatial resolution and high sample throughput analysis, the washout time should be as short as possible for the designed signal-smoothing device. Compared to that without the wave stabilizer, the washout time is increased by 1 and 2 s for signal decay of approximately 4 orders of magnitude with the wave stabilizer at positions B and A, respectively (Figure 3). This result indicates that the wave signal stabilizer has a limited effect on the washout time. In comparison with previously developed signal stabilizers such as the baffled-type stabilizer,[14] the cyclone-type stabilizer,[14] and the squid signal stabilizer,[11] this is an important advantage for our designed wave signal stabilizer.

Effect on the Signal Intensity. Figure 4 shows the normalized signal intensities of 63 elements (relative to those without the stabilizer) at different test times. These signals were produced using a laser ablation repetition rate of 6 Hz lasting 50 s at a spot size of 44 μm on the glass standard NIST SRM 610. It would be better if the designed wave stabilizer device did not affect the signal intensity or remove aerosols in an elementally selective way. It can be seen that most of the normalized elemental signals lie within the range of 0.95−1.0. Compared with previously developed signal stabilizers, such as the baffled-type stabilizer,[14] the cyclone-type stabilizer,[14] and the wire signal stabilizer,[6] this is an important advantage for the designed wave signal stabilizer. ^{66}Zn, ^{103}Rh, ^{111}Cd, ^{121}Sb, ^{126}Te, and ^{195}Pt are significant exceptions. The normalized signals of ^{66}Zn, ^{111}Cd, ^{121}Sb, and ^{126}Te are consistently lower (lie within

DOI: 10.1021/ac503749k
Anal. Chem. 2015, 87, 1152−1157

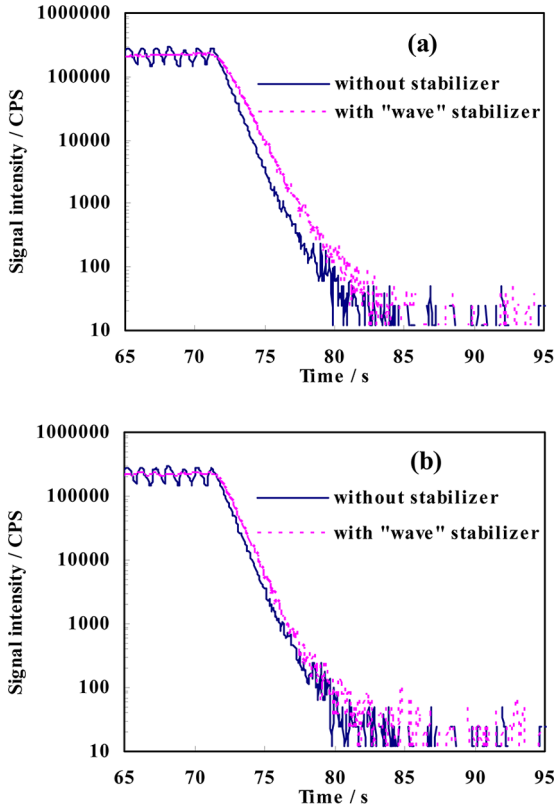

Figure 3. Comparison of the aerosol washout time after 50 s of laser ablation without and with the wave signal-smoothing device at position A (a) and position B (b).

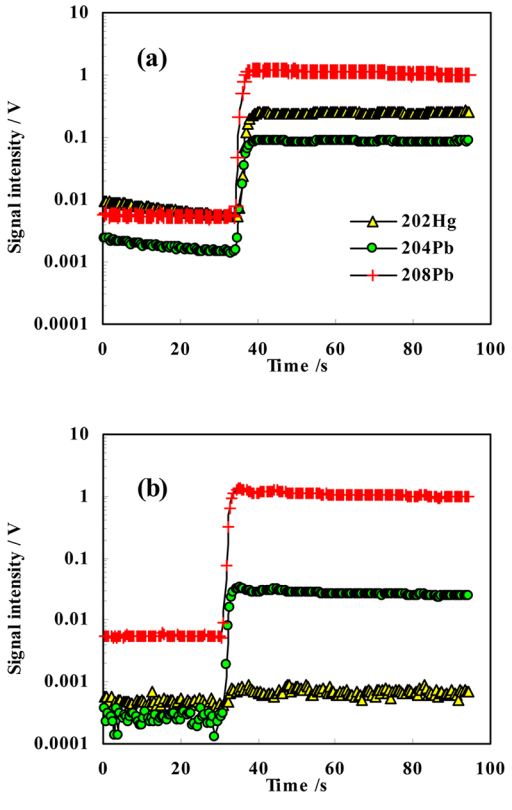

Figure 5. Signal profiles of ^{202}Hg, ^{204}Hg + ^{204}Pb, and ^{208}Pb produced by continuous laser ablation without (a) and with (b) the wave signal-smoothing device. Signals were acquired using a repetition rate of 6 Hz and a spot size of 44 μm in sulfide standard MASS-1.

the range of 0.90−0.95) when measured at different times. The reason for this is unclear. Further work on Zn, Cd, Sb, and Te deposition is needed to identify the specific mechanisms. The large variation ranges for ^{103}Rh and ^{195}Pt (0.93−1.16) may be related to their heterogeneous distribution in NIST 610 glass.[23,24] These results suggest that the wave stabilizer does not significantly affect the aerosol transport efficiency and remove aerosols in an elementally selective way for the operating conditions used in this study.

Removing Hg from the Carrier Gas and the Sample Aerosol. Figure 5 shows the ^{202}Hg, ^{204}Pb, and ^{208}Pb signal profile produced by laser ablation of the MASS-1 sulfide standard at a repetition rate of 8 Hz with and without the wave device at position A using MC-ICPMS. It can be seen that the gas background of mercury in LA-MC-ICPMS is reduced from 6 to 0.5 mV by using the wave device. This reduction is important for Pb isotope and U−Pb dating analysis in samples with a low Pb content using LA-MC-ICPMS. The mercury content is 57 μg g^{-1} in MASS-1. The laser ablation produced ^{202}Hg signal intensity in MASS-1 is 256 and 0.7 mV without and with the wave device, respectively. A reduction factor of 366 for the ^{202}Hg signal was obtained. This result suggests that the Hg is also almost completely removed from the laser ablation produced sample aerosol particles. In contrast, the signal intensities of ^{208}Pb are similar both with and without the wave device. We propose that Hg is enriched and transported primarily in the small particulate form due to its volatility and hence can interact well with the gold coating on the surfaces of the different corrugated plates in the smoothing elements and

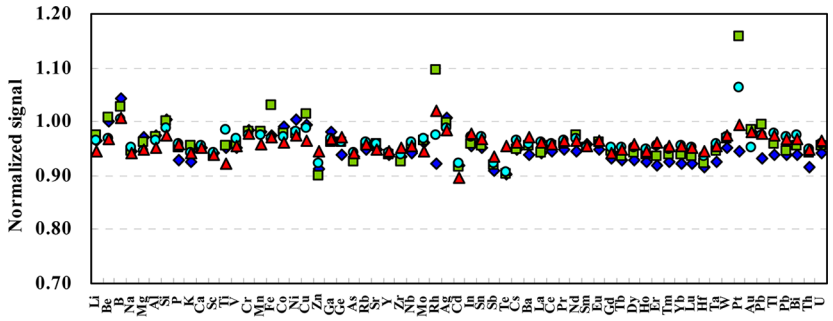

Figure 4. Signal intensities of 63 elements obtained with the wave signal stabilizer normalized to conditions without the wave signal stabilizer by using a laser ablation repetition rate of 6 Hz lasting 50 s with a spot size of 44 μm in NIST SRM 610. Different symbol colors mean different test times.

DOI: 10.1021/ac503749k
Anal. Chem. 2015, 87, 1152−1157

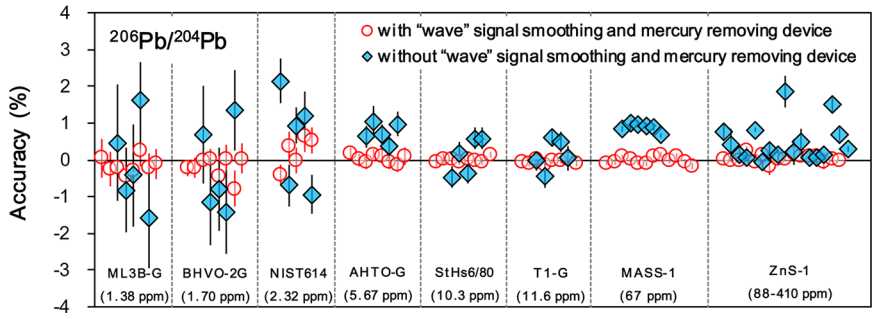

Figure 6. Relative deviation of the determined $^{206}Pb/^{204}Pb$ isotope ratios in glass standards, sulfide standard MASS-1, and natural sphalerite ZnS-1 from reference values both with and without the wave signal-smoothing and mercury-removing device. Each data point represents one single-spot analysis with a spot size of 90 μm. Error bars represent the within-run precision (2σ) for single-spot analysis. For glass standards analysis, the ^{202}Hg and $^{204}Hg + {}^{204}Pb$ signals are detected by using ion counters. For the sulfide standard MASS-1 and natural sphalerite ZnS-1, ^{202}Hg and $^{204}Hg + {}^{204}Pb$ were measured using Faraday cups. The reference values used are taken from the GeoReM database (http://georem.mpch-mainz.gwdg.de/).

the inner surface of the stainless steel cylinder compared to other more refractory elements such as Pb, which are transported predominantly as normal solid aerosol particles. However, the mechanisms that cause this effect need further investigation.

Application to Lead Isotope Analysis. Lead isotopes have been widely applied for the fingerprinting and identification of geological processes.[17,18] LA-MC-ICPMS is one of the most powerful tools for lead isotopic analysis.[15−18] The low abundance of ^{204}Pb (~1.4% of all common Pb) and the isobaric interference of ^{204}Hg from the carrier gas and samples are considered to be the main problems in obtaining high-precision measurements of $^{206/207/208}Pb/^{204}Pb$ by using LA-MC-ICPMS. Figure 6 shows the relative deviation of the determined $^{206}Pb/^{204}Pb$ isotope ratios in glass standards (ML3B-G, BHVO-2G, NIST SRM 614, AHTO-G, StHs6/80, T1-G), sulfide standard MASS-1, and natural sphalerite ZnS-1 from reference values both with and without the wave device. It can be seen from Figure 6 that the agreement between our data obtained with the wave device was much better than that between the data obtained without the mercury-removing device. This is particularly true for low Pb content samples ML3B-G ([Pb] = 1.38 $\mu g\ g^{-1}$), BHVO-2G ([Pb] = 1.70 $\mu g\ g^{-1}$), NIST SRM 614 ([Pb] = 2.32 $\mu g\ g^{-1}$), and AHTO-G ([Pb] = 5.67 $\mu g\ g^{-1}$). For high Hg content sample MASS-1 ([Hg] = 57 $\mu g\ g^{-1}$), the determined $^{206}Pb/^{204}Pb$ values are consistently higher than the reference value by 1% without use of the wave signal-smoothing and mercury-removing device. Excellent agreement between the determined values and the reference value in MASS-1 is obtained by using our developed mercury-removing device. The $^{206}Pb/^{204}Pb$ isotope ratios determined in natural sphalerite ZnS-1 are scattered for different laser ablation spot analyses without the wave device because the Hg and Pb contents are highly varied for different laser ablation sampling locations in natural sphalerite sample ZnS-1 ($^{204}Hg/^{204}Pb$ = 0.186−6.419). By using our mercury-removing device, the $^{206}Pb/^{204}Pb$ isotope ratios determined in different laser ablation sampling locations in natural sphalerite sample ZnS-1 are very consistent. These results demonstrate that the wave device that we have developed is well suited for lead isotope analysis in low Pb content samples and/or high Hg content samples.

CONCLUSIONS

The wave signal-smoothing and mercury-removing device that we developed is able to provide smooth signals even at a low laser repetition rate of 1 Hz, which makes it well suited for routine optimization of LA-ICPMS and LA-MC-ICPMS as well as low repetition rate laser ablation analysis. Not only was the mercury in the carrier gas effectively removed, but also the mercury in the laser ablation produced sample aerosols was significantly removed. This reduction of the mercury signal is important for lead isotopes and for U−Pb dating analysis by LA-MC-ICPMS, where low ^{204}Hg signals are necessary for precise and accurate analyses. The developed wave signal-smoothing and mercury-removing device has been used successfully for lead isotope analysis in low Pb content samples, as well as in high Hg content samples.

AUTHOR INFORMATION

Corresponding Author

*E-mail: zchu@vip.sina.com. Phone: +86 27 61055600. Fax: +86 27 67885096.

Notes

The authors declare no competing financial interest.

ACKNOWLEDGMENTS

We thank Klaus Peter Jochum for providing MPI-DING reference glasses. Thoughtful comments by Reinhard Niessner and two anonymous reviewers have significantly improved the manuscript. This research is supported by the National Natural Science Foundation of China (Grants 41273030, 41322023, and 41373026), the Fundamental Research Funds for National Universities, the CERS-China Equipment and Education Resources System (Grant CERS-1-81), the State Administration of the Foreign Experts Affairs of China (Grant B07039), the Opening Foundation of the Beijing SHRIMP Center (National Science and Technology Infrastructure), and the MOST Special Fund from the State Key Laboratory of Geological Processes and Mineral Resources.

REFERENCES

(1) Russo, R. E.; Mao, X. L.; Liu, H. C.; Gonzalez, J.; Mao, S. S. *Talanta* **2002**, *57*, 425−451.
(2) Günther, D.; Hattendorf, B. *TrAC, Trends Anal. Chem.* **2005**, *24*, 255−265.
(3) Shaheen, M. E.; Gagnon, J. E.; Fryer, B. J. *Chem. Geol.* **2012**, *330−331*, 260−273.
(4) Orellana, F. A.; Gálvez, C. G.; Orellana, F. A.; Gálvez, C. G.; Roldán, M. T.; García-Ruiz, C.; Roldán, M. T.; García-Ruiz, C. *TrAC, Trends Anal. Chem.* **2013**, *42*, 1−34.
(5) Bleiner, D.; Günther, D. *J. Anal. At. Spectrom.* **2001**, *16*, 449−456.

DOI: 10.1021/ac503749k
Anal. Chem. 2015, 87, 1152−1157

(6) Hu, Z. C.; Liu, Y. S.; Gao, S.; Xiao, S. Q.; Zhao, L. S.; Günther, D.; Li, M.; Zhang, W.; Zong, K. Q. *Spectrochim. Acta, Part B* **2012**, *78*, 50−57.
(7) Cottle, J. M.; Horstwood, M. S. A.; Parrish, R. R. *J. Anal. At. Spectrom.* **2009**, *24*, 1355−1363.
(8) Mank, A. J. G.; Mason, P. R. D. *J. Anal. At. Spectrom.* **1999**, *14*, 1143−1153.
(9) Schilling, G. D.; Andrade, F. J.; Barnes, J. H.; Sperline, R. P.; Denton, M. B.; Barinaga, C. J.; Koppenaal, D. W.; Hieftje, G. M. *Anal. Chem.* **2007**, *79*, 7662−7668.
(10) Liu, Y. S.; Hu, Z. C.; Yuan, H. L.; Hu, S. H.; Chen, H. H. *J. Anal. At. Spectrom.* **2007**, *22*, 582−585.
(11) Müller, W.; Shelley, M.; Miller, P.; Broude, S. *J. Anal. At. Spectrom.* **2009**, *24*, 209−214.
(12) Fricker, M. B.; Kutscher, D.; Aeschlimann, B.; Frommer, J.; Dietiker, R.; Bettmer, J.; Günther, D. *Int. J. Mass Spectrom.* **2011**, *307*, 39−45.
(13) Gurevich, E. L.; Hergenröder, R. *J. Anal. At. Spectrom.* **2007**, *22*, 1043−1050.
(14) Tunheng, A.; Hirata, T. *J. Anal. At. Spectrom.* **2004**, *19*, 932−934.
(15) Woodhead, J.; Hergt, J.; Meffre, S.; Large, R. R.; Danyushevsky, L.; Gilbert, S. *Chem. Geol.* **2009**, *262* (3−4), 344−354.
(16) Souders, A. K.; Sylvester, P. J. *J. Anal. At. Spectrom.* **2010**, *25* (7), 975−988.
(17) Darling, J. R.; Storey, C. D.; Hawkesworth, C. J.; Lightfoot, P. C. *Geochim. Cosmochim. Acta* **2012**, *99*, 1−17.
(18) Standish, C.; Dhuime, B.; Chapman, R.; Coath, C.; Hawkesworth, C.; Pike, A. *J. Anal. At. Spectrom.* **2013**, *28* (2), 217−225.
(19) Hirata, T.; Nesbitt, R. W. *Geochim. Cosmochim. Acta* **1995**, *59*, 2491−2500.
(20) Jackson, S. E.; Pearson, N. J.; Griffin, W. L.; Belousova, E. A. *Chem. Geol.* **2004**, *211*, 47−69.
(21) Hirata, T.; Iizuka, T.; Orihashi, Y. *J. Anal. At. Spectrom.* **2005**, *20*, 696−701.
(22) Zhang, L.; Ren, Z. Y.; Nichols, A. R. L.; Zhang, Y. H.; Zhang, Y.; Qian, S. P.; Liu, J. Q. *J. Anal. At. Spectrom.* **2014**, *29*, 1393−1405.
(23) Eggins, S. M.; Shelley, J. M. G. *Geostand. Newsl.* **2002**, *26*, 269−286.
(24) Hu, Z. C.; Liu, Y. S.; Li, M.; Gao, S.; Zhao, L. S. *Geostand. Geoanal. Res.* **2009**, *33*, 319−335.

DOI: 10.1021/ac503749k
Anal. Chem. 2015, 87, 1152−1157